Fluorescence quenching and photobleaching in Au/Rh6G nanoassemblies: impact of competition between radiative and non-radiative decay

L. Dong lindong@kth.se — Royal Institute of Technology, Division of Optics, 164 40 Kista, Sweden
F. Ye — Royal Institute of Technology, Division of Functional Materials, 164 40 Kista, Sweden
J. Hu — Royal Institute of Technology, Division of Optics, 164 40 Kista, Sweden; Zhejiang University, Center for Optical and Electromagnetic Research, 310058 Hangzhou, China
S. Popov — Royal Institute of Technology, Division of Optics, 164 40 Kista, Sweden
A. T. Friberg — Royal Institute of Technology, Division of Optics, 164 40 Kista, Sweden; Aalto University, Department of Applied Physics, 00076 Aalto, Finland; University of Eastern Finland, Department of Physics and Mathematics, 80101 Joensuu, Finland
M. Muhammed — Royal Institute of Technology, Division of Functional Materials, 164 40 Kista, Sweden

We report the study of fluorescence quenching from nanoassemblies formed by Rhodamine 6G and gold nanoparticles (Au NPs) of 2.6 nm radius. The presence of Au NPs induces long-term degradation of the photostability (photobleaching) of Rhodamine 6G used as a gain medium in a Fabry-Perot laser cavity. We found that the degradation gets profound when the Au NPs concentration is significantly increased. Calculation of the radiative rate and direct time-resolved measurement of the fluorescence decay indicates that both the decrease of radiative decay rate and increase of non-radiative decay rate are responsible for the fluorescence quenching and photostability degradation. An energy transfer from the dye molecules to gold nanoparticles is dominating within small distance between them and suppresses the quantum efficiency of Rhodamine 6G drastically. In a long time scale, the photobleaching rate was slowing down, and the laser output intensity reached a stabilized level which depends on the gold nanoparticles concentration. [DOI: 10.2971/jeos.2011.11019]

Keywords: gold nanoparticles, Rhodamine 6G, fluorescence quenching, photostability

1 INTRODUCTION

Interaction between fluorophore (dye, quantum dots) and noble metal nanoparticles (NPs) has been intensively investigated in recent years for applications in optical materials, biosensing and scanning probe microscopy [1]-[4]. There were reports showing that both the enhancement and deterioration of fluorophore emission intensity can be introduced by gold NPs, depending on the size and shape of the NPs, the orientation of the fluorophore's molecular dipole moment, and the overlap of the fluorophore emission spectrum with the spectrum of metal NPs' surface plasma resonance. Enhancement with a factor more than 2000 times was observed with fluorophore Rose Bengal spun on a quartz plate with immobilized spherical gold NPs (100 nm diameter) [5]. Meanwhile, significant fluorescence quenching was also observed for molecules of Lissamine attached to 1 nm radius NPs via a thioether group [6]. It is believed that both enhancement and quenching exist simultaneously in the same fluorophore-nanoparticle mixture depending on the distances between the fluorophore and NPs. For distances r smaller than 10 nm, an energy transfer, with the rate proportional to $1/r^6$ (namely Förster Resonant Energy Transfer, or FRET), from the fluorophore molecules in excited state to the metal NPs is dominating over the fluorescence enhancement by the surface plasma resonance [7]. Fluorescence quenching is most likely to take place within such a range of distances.

Besides the enhancement, the fluorescence quenching is of strong interest for many applications. Specifically, within small distances between the dye and nanoparticles fluoresce quenching due to FRET is dominating over fluorescence enhancement. This feature is highly important for applications in scanning probe microscopy, surface enhanced Raman spectroscopy and biosensing etc [4, 8]. For example, fluorescence quenching by gold NPs has been applied to improve the contrast in scanning probe microscopy and to recognize biomolecules [4]. High-rate controllable fluorescence quenching is an interesting alternative to increase the efficiency of solar cells [9].

In recent study, Karthikeyan investigated fluorescence quenching of Rhodamine 6G in Au nanocomposite polymers and found that the fluorescence decay rate of Rhodamine 6G

Received January 14, 2011; published April 22, 2011 ISSN 1990-2573

changes because of the presence of Au NPs, and this change depends on the particle size [10]. An impact of the variation of gold NP concentration was studied by Zhu et al. [11]. In that report, a NP radius of 20 nm was chosen, which is outside the FRET dominated region. The authors modeled the nanostructure as a metal core with concentric shell of dye molecules and calculated the field enhancement factor. Much less is known about how the NP concentration influences the fluorescence properties of dye molecules which interact with NPs of the size smaller than 10 nm.

In the present work, we focus on gold/Rhodamine 6G clusters in liquid solution instead of solid matrices. We kept the dye concentration in the solution constant and varied the concentration of Au NPs within different orders of magnitude. Our interest is targeted on gold NPs with the size of ~5 nm. Because of the $1/r^6$ dependence of the FRET efficiency, we expect that a dramatic variation in both the radiative and non-radiative decay rate can give more information about the physical mechanism behind the influence of Au NPs' on fluorescence of dye molecules. Moreover, we also investigated the photobleaching property of the Au/dye solution placed into a laser cavity and optically pumped by a series of laser pulses over a relatively long time period. This property is important for lasing applications using organic dyes as the gain medium. Using radiative decay rate calculation and direct time-resolved measurement of the fluorescence decay rate, we introduce and consider a generalized relation between the radiative/non-radiative decay and the photobleaching.

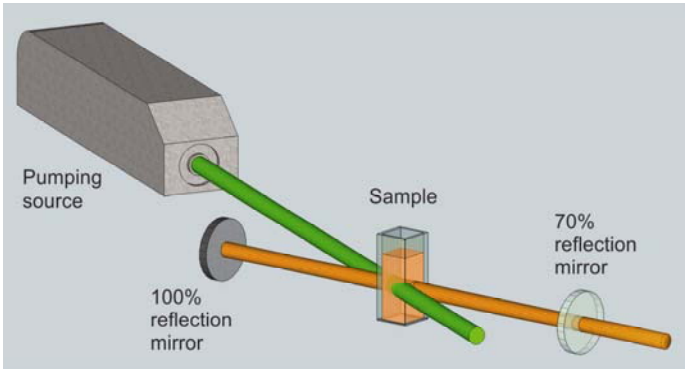

FIG. 1 Schematics of experimental setup for photobleaching measurement.

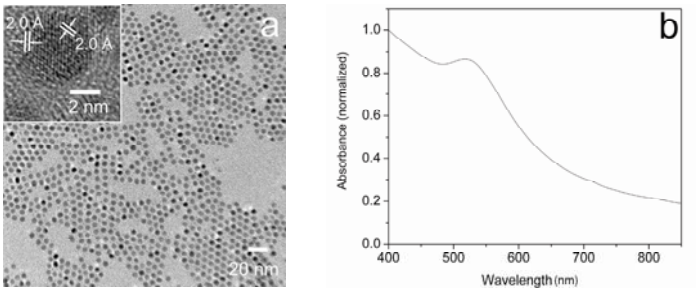

FIG. 2 a) TEM image and b) UV-Vis absorbance spectrum (normalized) of Au NPs in dispersion of $CHCl_3$.

2 EXPERIMENTAL DETAILS

Synthesis of gold NPs with a wide range of sizes and shapes has been reported in earlier studies [12, 13]. In the present work, homogenous and small-sized Au NPs (~5 nm) were prepared using a modified Brust two phase method by reducing hydrochlorauric acid in mixture of water and chloroform [14]. Typically, 15 mL of $HAuCl_4$ (10 mg/mL) was mixed with 40 mL of chloroform containing 1.1g of tetraoctylammonium bromide. The solution was stirred vigorously for 30 min before addition of 120 μL of 1-dodecanethiol. Then 12.7 mL of aqueous solution of 192 mg of sodium borohydride was slowly added into the mixture. After continuously stirring for 3 hours, the layer of chloroform containing Au NPs was collected.

The morphology of Au NPs was characterized by JEM-2100F field emission transmission electron microscope (TEM) operating at accelerating voltage of 200 kV. PerkinElmer Lambda 750 UV-VIS Spectrometer was used to measure the absorbance of Au NPs in dispersion of chloroform. Concentration of gold was measured by inductively coupled plasma atomic emission spectroscope (ICP-AES) (Thermo Scientific iCAP 6500 series). The hydrodynamic size of the gold/Rhodamine 6G nanoassemblies in chloroform was measured by photon correlation spectroscopy (PCS) (Delsa™ Nano particle size analyzer, Beckman Coulter).

The sample for photostability experiment was prepared by mixing certain amount of gold NPs with 0.2 mM of Rhodamine 6G aqueous solution using ultrasonic concussion. The liquid sample was injected into a quartz cuvette with a volume of 0.5 mL. The cuvette was inserted in between two mirrors (100% reflection metal mirror and 70% reflection output coupling mirror) to form a 20 cm long laser cavity (Figure 1). The sample was longitudinally pumped with a 532 nm pulsed Nd:YAG laser, while the repetition rate of the pump laser can be adjusted from 1 to 22 Hz. The cavity output radiation was collected by a collimator and sent in to an optical spectrum analyzer through optical fiber. Fluorescence decay lifetime of the Au/Rhodamine 6G nanoassemblies in liquid solution was measured with a Hamamatsu streak camera. For this measurement, the sample in a cuvette was pumped with a pulsed Ti:sapphire laser with 400 nm output wavelength, 76 MHz repetition rate and 150 fs pulse duration.

3 RESULTS AND DISCUSSION

3.1 Morphology and hydrodynamic sizes of gold NPs

The TEM micrograph shows the morphology of Au NPs (Figure 2a)), and the particle radius is 2.6 ± 0.3 nm (average ± standard deviation). The high resolution TEM image reveals the single crystalline nature of these hydrophobic particles with the lattice spacing of ~2.0 Å, close to that of the Au (100) lattice plane (inset of Figure 2a)). UV-Vis measurement shows a characteristic absorption peak of the surface plasma resonance centered at 520 nm (Figure 2b)).

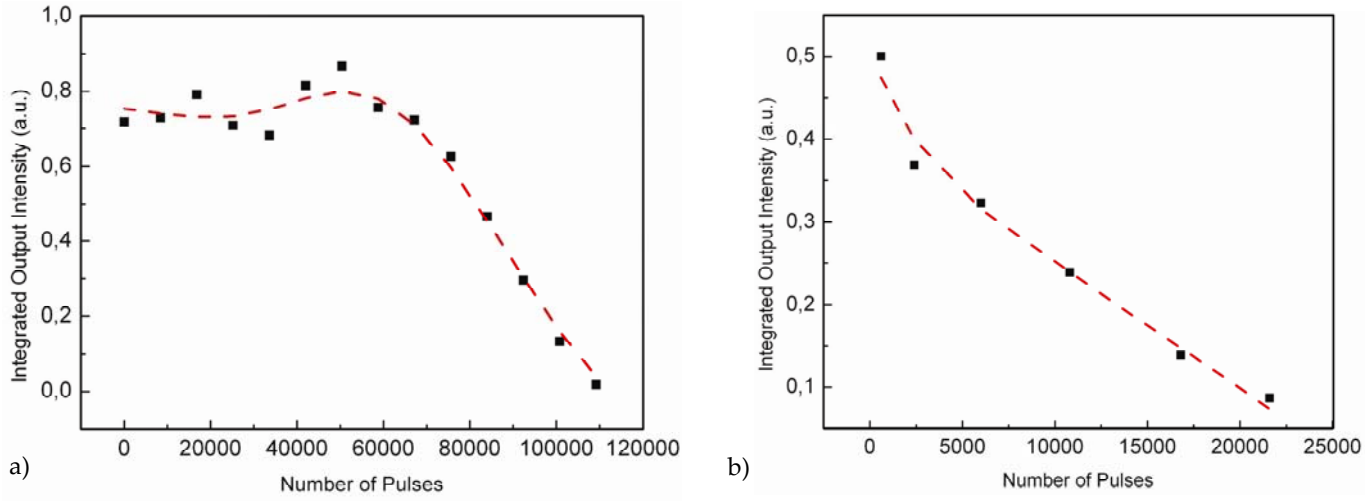

FIG. 3 Dependence of output intensity on the number of pulses with pump pulse energy of 12 mJ and repetition rate of 20 Hz for a) dye solution without Au NPs and b) gold/dye assemblies where the number of Au NPs is equal to the number of dye molecules.

Interactions of Au NPs and dye molecules in CHCl3 suspension were studied on their random movement, i.e. Brownian motion, by means of the PCS method. The hydrodynamic size distributions of the particles before and after mixing with dye molecules were obtained by PCS measurements. The average mean value of hydrodynamic diameters (volume distribution) of Au NPs in $CHCl_3$ is 116 nm, which is much bigger than particle size obtained by TEM. This is because hydrodynamic diameter includes the size of the core (Au NP) and thickness of diffusion layer on the core, while the TEM measurement only gives the information about core particles. The diffusion layer is composed of stretched surfactant molecules on the surface of particles and some solvent molecules moved together with the particles instead of mixing in the bulk solution. When 0.2 mM Rhodamine 6G solution was mixed with same amount of Au NPs (defined as Au = 100%), the hydrodynamic size of particles increased to 159 nm, which indicated the formation of Au/Rhodamine 6G nanoassemblies, and the size increase was due to the attached dye molecules. When 1% amount of Au NPs was mixed with the same concentrated dye solution (defined as Au = 1%), hydrodynamic size was obtained as 172 nm, and the increased particle size indicated immobilization of more dye molecules on each Au NPs.

3.2 Photostability

In this section, first we describe the time varied fluorescence quenching of dye solution without gold NPs. The relative (normalized) measurement of the output laser intensity is shown in Figure 3a). The sample was pumped with laser pulses of 20 Hz repetition rate and 12 mJ pulse energy, providing about 4 mJ of the output with a fresh solution. It is seen that the output intensity is stable between 0.6 and 0.8 for the first 60000 pulses. After that, the output intensity decreases almost linearly until it reaches the very low level. Next, we measured the time varied fluorescence quenching of Au/dye solution with the concentration Au=100% under the same pump condition. The result is shown in Figure 3b). The output intensity at the beginning shows a ~20% quenching compared with a pure dye solution, which demonstrates the deterioration effect introduced by the small-sized gold NPs. Moreover, the output intensity drops from the very beginning in a linear trend without signs of stabilization as in Figure 3a). The photobleaching rate is much higher than that of the pure dye solution.

As the next step, we measured and compared the time varied fluorescence quenching of Au/dye solutions with different Au NPs concentrations (Figure 4). Pump pulse energy was 12 mJ and repetition rate was 2 Hz. One can see that the high NP concentration results in a lower output intensity during the whole processes (Figure 4a)), indicating a lower radiative rate of the dye. A normalized plot reveals that a higher NP concentration gives an increased photobleaching rate at the beginning of the measurement (Figure 4b)). This is consistent with the condition of pure dye solution without NPs, where the bleaching rate of zero was found at the beginning, i.e. the stable period for the first 60000 pulses. Therefore, it is reasonable to assume that the presence of Au NPs of particular size speeds up the photobleaching of dye molecules. Especially with a higher concentration, the Au NPs are more likely to migrate closer to dye molecules and deactivate the latter efficiently. As another feature, we found that the output intensities of the two samples reach a similar level at the end (for normalized condition, Figure 4b)), and the photobleaching rates slow down to nearly zero. Certain dynamic equilibrium may be built up between dye molecules' acquiring and dissipating energy, with the presence of Au NPs. It might indicate that the bleaching induced by the Au NPs may differ from the intrinsic photobleaching of pure dye, which is a dynamic process where Au NPs attract and release dye molecules simultaneously rather than a non-reversible process.

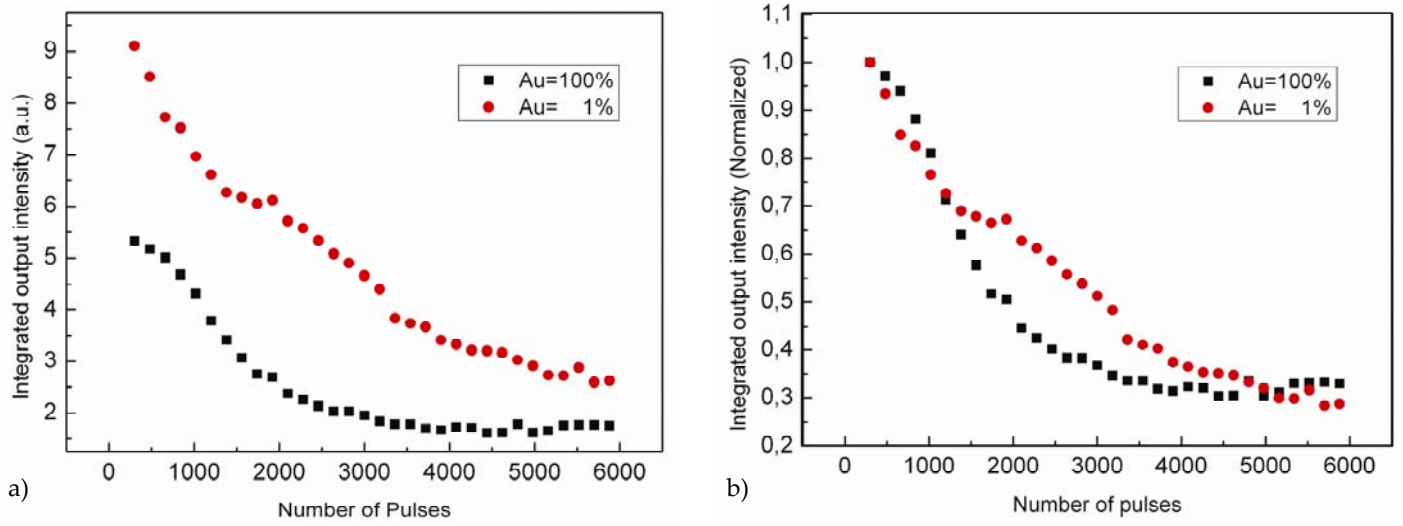

FIG. 4 Dependence of output intensity on the number of pulses with pump pulse energy of 12 mJ and repetition rate of 2 Hz in a) un-normalized scale and b) normalized scale. The black squares are correspondent to gold/dye assemblies where the number of Au NPs is equal to the number of dye molecules (Au = 100%). The red dots are correspondent to gold/dye assemblies where the number of Au NPs is 1% of the number of dye molecules (Au = 1%).

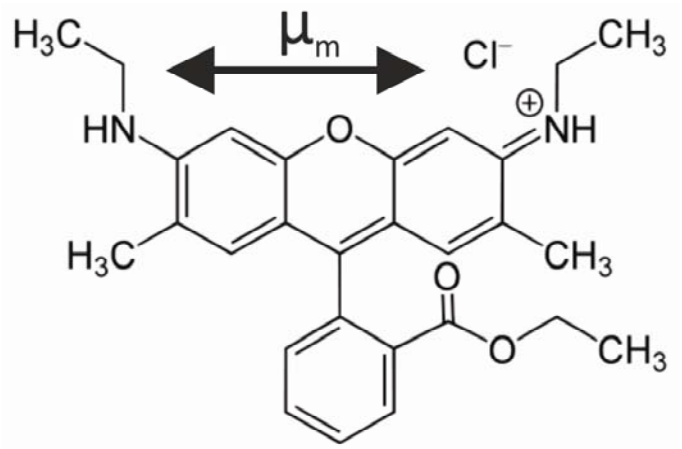

FIG. 5 Schematic molecular structure of Rhodamine 6G. The arrows show the direction of the molecular dipole moment along the three adjacent benzene rings.

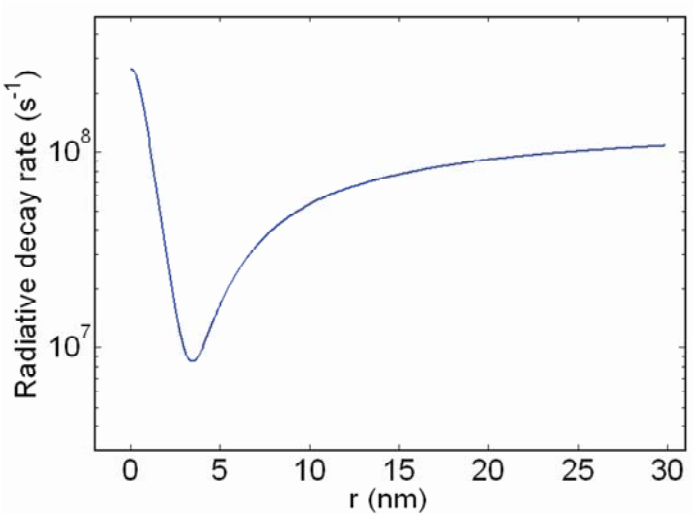

FIG. 6 Calculated radiative decay rate of Rhodamine 6G in Au/dye nanoassemblies with different Au NPs radii, based on the Gersten-Nitzan model.

3.3 Radiative and non-radiative decay rate analysis

The influence of the metal NPs on the radiative and non-radiative decay rate of the fluorophore makes up two of the three major metal-fluorophore interactions. (The other one is the strengthening of the excitation light field by the metal [15]). Thus, an analysis of the radiative and the non-radiative decay rate variation is helpful to get a deeper understanding of the quenching and photobleaching mechanism. The Gersten-Nitzan model provides a useful tool for such a purpose [16]. Even though the prediction of non-radiative rate by this model still shows discrepancy with the experimental results, the prediction on radiative rate is almost perfect [6]. Based on this, we applied the model to calculate the radiative decay rate for the particular scenario in this work. Several precautions concerning the key parameters and conditions in the model were taken during the calculation. First, the orientation of the molecular dipole of Rhodamine 6G was treated as perpendicular to the Au NPs' surfaces. This is because the Rhodamine 6G molecules are conjugated with the Au NPs by the amine group and the dipole moment is along the three adjacent benzene rings (Figure 5) [17]. Secondly, the polarizability of Rhodamine 6G was taken from a wavelength dependent function [18] instead of a constant. The calculation result is shown in Figure 6. There is an 18-fold drop of the radiative rate due to the existence of the 2.6 nm radius Au NPs. This can be directly translated into a pronounced suppress of the quantum efficiency (originally was as high as 0.95) for Rhodamine 6G and fluorescence quenching as a result. However, the experimentally measured radiative rate dropped only by 2 times (Figure 7). In this time-resolved decay rate measurement, the intensity at zero time I (t = 0) was a direct measure of the radiative decay rate R_{rad} by the relation $R_{rad} = gI$ (t = 0) where g is a constant related to the photon collection efficiency of the system. The discrepancy between the calculation and the experimental results indi-

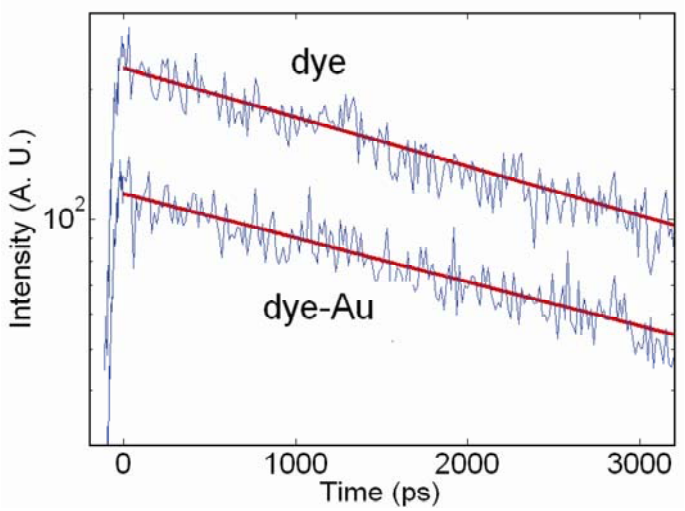

FIG. 7 Time-resolved fluorescence spectra of the pure Rhodamine 6G solution and the Au/Rhodamine 6G assemblies with Au = 1%.

cates that only part of the dye molecules are attached to the Au NPs. Meanwhile, there is a slight increase of the fluorescence decay time from 3.8 ns for the pure dye solution to 4.2 ns for the Au/dye assemblies. The 3.8 ns decay time of pure dye solution agrees well with the value found in literature where the decay time for Rhodamine 6G solution of the same concentration was measured [19]. Since the fluorescence decay rate is just the sum of the radiative and non-radiative decay rates, a drastic decrease in the radiative decay rate together with a slight decrease in the fluorescence decay rate means a considerable increase of the non-radiative decay rate. If we also take into account the high quantum efficiency of 0.95 for Rhodamine 6G (R_{rad}:$R_{non\text{-}rad}$ = 19:1), then one can conclude that the increase in the non-radiative decay rate is pronounced. Due to the low concentration (0.2 mM), it is unlikely that dimers of Rhodamine 6G molecules are formed [19]. Therefore, the increase in the non-radiative decay rate is most probably due to the energy transfer between the dye molecules and the Au NPs, i.e. the FRET. For the Au = 100% assembly, the radiative decay rate decreases even further such that the time-resolved spectrum (not presented in this paper) is overwhelmed in the noises and fluorescence lifetime cannot be extrapolated from it. Comparing these three samples, it is suggested that the photobleaching property of Au/Rhodamine 6G assemblies is closely related to the ratio of $R_{rad}/R_{non\text{-}rad}$ at the beginning of the measurement. The higher the ratio, the smaller bleaching tendency with time. The role played by the energy transfer from dye molecules to Au NPs is equivalent to the conventional photobleaching mechanism in pure dye solutions, i.e. to convert radiatively recombined excitons to those recombined non-radiatively. In other words, the FRET provides an extra channel for non-radiative decay. The capacity of this channel is related to the Au NPs concentration. The photobleaching rate decreases with time and approaches zero after several thousands of pump pulses, when the new equilibrium in terms of energy acquiring (from the pump source) and dissipating (both radiative and non-radiative) is built up for the dye molecules. Therefore, the level at which the equilibrium stays, i.e. the output intensity at the end of the photobleaching measurement, is dependent on the concentration of the Au NPs.

4 CONCLUSION

In this work, we investigated the impact of colloidal gold NPs with variable concentrations on the quenching of the dye fluorescence in Au/Rhodamine 6G nanoassemblies. The effect is mainly attributed to the FRET due to small size of Au NPs. The dye-NP solution placed in a laser cavity demonstrated faster photobleaching dynamic of this gain material in comparison with a pure dye. However, in a long time scale, e.g. after 4000 pulses of pumping, increased concentration of Au NPs leads to diminishing of the photobleaching rate. The lasing output intensity with such a gain material achieves its stabilized level faster than for the pure dye solution. A comparison between the calculated and experimentally measured radiative decay rate revealed that not all dye molecules were attracted in the vicinity of NPs, which is not obviously seen for solutions with high Au NPs' concentration. It indicates that dynamic equilibrium between energy acquiring and dissipating of dye molecules was achieved after the photobleaching rate was minimized.

References

[1] J. Zhang, Y. Fu, and J. R. Lakowicz, "Emission behavior of fluorescently labeled silver nanoshell: enhanced self-quenching by metal nanostructure" J. Phys. Chem. C **111**, 1955-1961 (2007).

[2] T. Uwada, R. Toyota, H. Masuhara, and T. Asahi, "Single particle spectroscopic investigation on the interaction between exciton transition of cyanine dye J-aggregates and localized surface plasmon polarization of gold nanoparticles", J. Phys. Chem. C **111**, 1549-1552 (2007).

[3] M. Fukushima, H. Yanagi, S. Hayashi, N. Suganuma, and Y. Taniguchi, "Fabrication of gold nanoparticles and their influence on optical properties of dye-doped sol-gel films" Thin Solid Films **438-439**, 39-43 (2003).

[4] M. De, P. S. Ghosh, and V. M. Rotello, "Applications of nanoparticles in biology" Adv. Mater. **20**, 4225-4241 (2008).

[5] T. Nakamura, and S. Hayashi, "Enhancement of dye fluorescence by gold nanoparticles: analysis of particle size dependence" Jpn. J. Appl. Phys. **44**, 6833-6837 (2005).

[6] E. Dulkeith, A. C. Morteani, T. Niedereichholz, T. A. Klar, J. Feldmann, S. A. Levi, F. C. J. M. van Veggel, D. N. Reihoudt, M. Moller, and D. I. Gittins, "Fluorescence quenching of dye molecules near gold nanoparticles: radiative and nonradiative effects" Phys. Rev. Lett. **89**, 203002-203005 (2002).

[7] T. Sen, S. Sadhu, and A. Patra, "Surface energy transfer from Rhodamine 6G to gold nanoparticles: a spectroscopic ruler" Appl. Phys. Lett. **91**, 043104-043104-3 (2007).

[8] J. M. Friedman, and R. M. Hochstrasser, "The use of fluorescence quenchers in resonance Raman spectroscopy" Chem. Phys. Lett. **33**, 225-227 (1975).

[9] M. Zorn, S. A. L. Weber, M. N. Tahir, W. Tremel, H.-J. Butt, R. Ber-

ger, and R. Zentel, "Light induced charging of polymer functionalized nanorods" Nano Lett. **210**, 2812-2816 (2010).

[10] B. Karthikeyan, "Fluorescence quenching of Rhodamine-6G in Au nanocomposite polymers" J. Appl. Phys **108**, 084311-084311-5 (2010).

[11] J. Zhu, K. Zhu, and L. Huang, "Using gold colloid nanoparticles to modulate the surface enhanced fluorescence of Rhodamine B" Phys. Lett. A **372**, 3283-3288 (2008).

[12] H. Vallhov, J. Qin, S. M. Johansson, N. Ahlborg, M. Muhammed, A. Scheynius, and S. Gabrielsson, "The importance of an endotoxin-free environment during the production of nanoparticles used in medical applications" Nano Lett. **6**, 1682-1686 (2006).

[13] F. Ye, H. Vallhov, J. Qin, E. Daskalaki, A. Sugunan, M. S. Toprak, A. Fornara, S. Gabrielsson, A. Scheynius, and M. Muhammed, "Synthesis of high aspect ratio gold nanorods and their effects on human antigen presenting dendritic cells" Int. J. Nanotechnol. In press.

[14] M. Brust, M. Walker, D. Bethell, D. J. Schiffrin, and R. Whyman, "Synthesis of thiol-derivatised gold nanoparticles in a two-phase liquid-liquid system" J. Chem. Soc., Chem. Commun. 801-802 (1994).

[15] J. R. Lakowicz, "Radiative decay engineering: biophysical and biomedical applications" Analytical Biochemistry **298**, 1-24 (2001).

[16] J. Gersten, and A. Nitzan, "Spectroscopic properties of molecules interacting with small dielectric particles", J. Chem. Phys. **75**, 1139-1152 (1981).

[17] M. A. Noginov, M. Vondrova, S. N. Williams, M. Bahoura, V. I. Gavrilenko, S. M. Black, V. P. Drachev, V. M. Shalaev, and A. Sykes, "Spectroscopic studies of liquid solutions of R6G laser dye and Ag nanoparticle aggregates" J. Opt. A: Pure Appl. Opt. **7**, S219 -S229 (2005).

[18] E. C. Le Ru, and P. G. Etchegoin, *Principle of Surface-Enhanced Raman Spectroscopy and Related Plasmonic Effects* (Elsevier, Oxford, 2009).

[19] K. A. Selanger, J. Falnes, and T. Sikkeland, "Fluorescence lifetime studies of Rhodamine 6G in methanol", J. Phys. Chem. **81**, 1960-1963 (1977).